Stabilization of Free Rigid Body Dynamics using a Single Internal Rotor: CDS205 Course Project

Dennice Gayme
dennice@caltech.edu

July 6, 2005

1 Introduction

A free rigid body with one rotor can be used as a model of satellite with one input. Stabilization of this type of body is of practical importance in analyzing the ability of a two or three rotor system to continue operation with one or more actuator failures as well as in understanding the capability of such a system to perform certain missions. This and similar systems have been extensively studied by the aerospace community in relation to spacecraft orientation, robotic devices, vehicle dynamics and other applications of rigid body motion, see the references in [2] for a detailed description of the applications of interest to the aerospace community.

There have been many papers discussing control of such a system as a model for satellite control and as a test case for the development of actuated rigid bodies such as the work described in [2], [3] and [4]. It is also an interesting system to study in terms of reduction theory and mechanical connections as in [6] and [7].

The paper of Bloch et. al [3] describes how to stabilize rotation of a free rigid body about its intermediate axis through the application of internal torque from one rotor placed its third principle axis, through an appropriate feedback law. Stability is proved using the energy-Casimir method. In this report the system is studied in the reduced space obtained in [6] and the results obtained in [3] are derived in more detail. A simulation of a rectangular free rigid body with a rotor on its third principle axis is carried out to verify the analytical results.

The paper is organized in the following manner; section (2) gives a brief overview of the system. Section (3) describes in detail the derivation of the system Lagrangian and the corresponding equations of motion. The Legendre transformation to Hamiltonian equations (Euler Poincaré Equations) is also provided in section (3). In section (4) the selection of an appropriate control law to stabilize the system about its intermediate axis is described. Also in

section (4) a stability proof based on the Energy Casimir method from [3] is re-derived. Then in section (5) the momentum spheres for various controller gains are shown to collaborate the analytical results. The final section of the paper outlines directions for future study.

2   System Description

The configuration (shape) space of a free rigid body with one internal rotor aligned with the third principle axis of the carrier body, as in [1] and [3] is $Q = SO(3) \times \mathbb{S}^1$. Where $SO(3)$ describes the rigid body's attitude (i.e. body coordinates in relation to the fixed reference frame) and $\mathbb{S}^1$ describes the rotor angle. The complete phase space of configurations and spatial momenta is $T^*SO(3) \times T^*\mathbb{S}^1$.

The reduced phase space as derived in a manner consistent with [3] and chapter 13 of [6] is $\mathfrak{so}(3)^* \simeq \mathbb{R}^3 \times \mathbb{R}$ and is identified with the body angular momenta $\mathbf{\Pi}$ and the conjugate momenta to the rotor angle.

Other properties of this system that are of interest are described in papers and books such as [1], [3], [7] and many others.

3   Equations of Motion

The kinetic energy of the system is derived by adding the kinetic energy of the free rigid body to the kinetic energy due to the addition of the internal rotor. There is no potential energy in the system, as it is assumed that the fixed (spatial) coordinate frame sits at the center of mass of the free rigid body and that the principle axis of the body are initially aligned with the coordinate frame. The body then rotates around in this coordinate frame and defines body coordinates that are related to the spatial coordinates through a rotation $\mathbf{R} \in SO(3)$ of each of the principle axes from the fixed frame. The kinetic energy of the system is computed based on the assumption, as in [6], that "the mass distribution of the body is described by a compactly supported density measure $\rho_0 d^3 X$ in the reference configuration."

Based on the foregoing assumptions the Lagrangian of the isolated (i.e. without the rotor) free rigid body in the body frame is (as in [6])

$$
\begin{aligned}
L &= \frac{1}{2} \int_{\mathcal{B}} \rho_0(X) \|\mathcal{V}(X,t)\|^2 d^3 X \\
&= \frac{1}{2} \int_{\mathcal{B}} \rho_0(X) \|\hat{\Omega} X\|^2 d^3 X
\end{aligned}
\tag{1}
$$

In (1), $\mathcal{V}(X,t)$ is the velocity of the rigid body in body coordinates and the spatial angular velocity, ω, (i.e. from the relation $v = \omega \times r = \hat{\omega} r$) is related to the body angular velocity, $\mathbf{\Omega}$, through the rotation matrix, $\mathbf{R} \in SO(3)$, that transforms body coordinates $\mathcal{X}$ to spatial (fixed) coordinates (i.e $x = \mathbf{R}\mathcal{X}$). The

explicit relationship, from [6], is;

$$\hat{\omega} = \mathbf{R}\hat{\Omega}\mathbf{R}^{-1}$$

One can then use the inner product defined in [6] as

$$\langle a, b \rangle = \int_{\mathcal{B}} \rho_0(X)(a \times X) \cdot (b \times X)d^3X \tag{2}$$

to simplify the expression (1) to

$$L(\mathbf{\Omega})_{carrier} = \frac{1}{2}\langle \mathbf{\Omega}, \mathbf{\Omega} \rangle \tag{3}$$

In this case one can compute the mass moment of inertia $\mathbf{I}_{carrier} = (I_1, I_2, I_3)$ for the free rigid body using an orthogonal basis $(\mathbf{E}_1, \mathbf{E}_2, \mathbf{E}_3)$ for the body coordinates using the following equation, from [6]

$$I_i = \mathbf{E}_i \cdot I\mathbf{E}_i = \int_{\mathcal{B}} \rho_0(X) \left(\|X\|^2 - (X^i)^2 \right) d^3X \tag{4}$$

As mentioned previously the expression in equation (2) represents the kinetic energy of only the free rigid body (or outer carrier without the rotor). In order to compute the Lagrangian for the total system the kinetic energy of the rotor must be added.

The kinetic energy of the rotor about the third principle axis of the free rigid body is

$$L(\mathbf{\Omega})_{rotor} = \frac{1}{2}\langle \mathbf{\Omega}_{rotor}, \mathbf{\Omega}_{rotor} \rangle \tag{5}$$

where $\mathbf{\Omega}_{rotor} = (\Omega_1, \Omega_2, \Omega_3 + \dot{\alpha})$, $\mathbf{\Omega} = (\Omega_1, \Omega_2, \Omega_3)$, is the body angular velocity of the carrier, α is the rotor angle and the moments of inertia for the rotor in about each axis are J_1, J_2, J_3.

The total system Lagrangian is:

$$L(\mathbf{\Omega})_{system} = \frac{1}{2}\left(\langle \mathbf{\Omega}, \mathbf{\Omega} \rangle + \langle \mathbf{\Omega}_{rotor}, \mathbf{\Omega}_{rotor} \rangle \right) \tag{6}$$

This can be expressed in components, as in [1]

$$L(\mathbf{\Omega})_{system} = \frac{1}{2}(\lambda_1 \Omega_1^2 + \lambda_2 \Omega_2^2 + I_3 \Omega_3^2 + J_3(\Omega_3 + \dot{\alpha})^2)$$

which is the rotational kinetic energy of the rigid body with $\lambda_i = I_i + J_i$. For the purpose of this report it is always assumed that $I_1 > I_2 > I_3$ and $J_1 = J_2$.

The Euler-Lagrange Equations, (called the Euler-Poincaré equations for generalized Rigid Body motion), can be computed from

$$\frac{d}{dt}\frac{\partial L}{\partial \mathbf{\Omega}} = \frac{\partial L}{\partial \mathbf{\Omega}} \times \mathbf{\Omega} \tag{7}$$

3

as described in [6]. Carrying out the computation yields

$$\frac{\partial L}{\partial \boldsymbol{\Omega}} = [\lambda_1 \Omega_1, \lambda_2 \Omega_2, \lambda_3 \Omega_3 + J_3 \dot{\alpha}]^T$$

$$\frac{\partial L}{\partial \boldsymbol{\Omega}} \times \boldsymbol{\Omega} = \begin{bmatrix} \lambda_2 \Omega_2 \Omega_3 - \Omega_2(\lambda_3 \Omega_3 + J_3 \dot{\alpha}) \\ \Omega_1(\lambda_3 \Omega_3 + J_3 \dot{\alpha}) - \lambda_1 \Omega_1 \Omega_3 \\ \lambda_1 \Omega_1 \Omega_2 - \lambda_2 \Omega_1 \Omega_2 \end{bmatrix}$$

$$\frac{d}{dt}\frac{\partial L}{\partial \boldsymbol{\Omega}} = \left[\lambda_1 \dot{\Omega}_1, \lambda_2 \dot{\Omega}_2, \lambda_3 \dot{\Omega}_3 + J_3 \ddot{\alpha}\right]^T$$

Finally the Euler-Poincaré equations of motion are:

$$\begin{aligned} \lambda_1 \dot{\Omega}_1 &= \lambda_2 \Omega_2 \Omega_3 - \Omega_2(\lambda_3 \Omega_3 + J_3 \dot{\alpha}) \\ \lambda_2 \dot{\Omega}_2 &= -\lambda_1 \Omega_1 \Omega_3 + \Omega_1(\lambda_3 \Omega_3 + J_3 \dot{\alpha}) \\ \lambda_3 \dot{\Omega}_3 + J_3 \ddot{\alpha} &= \lambda_1 \Omega_1 \Omega_2 - \lambda_2 \Omega_1 \Omega_2 \\ \dot{l}_3 &= u \end{aligned} \tag{8}$$

The conjugate (angular) momenta, to each Ω_i $i = 1, 2, 3$ are given by the Legendre transformation as $\Pi_i = \frac{\partial L}{\partial \Omega_i}$. Similarly the conjugate momentum to $\dot{\alpha}$ is $l_3 = \frac{\partial L}{\partial \dot{\alpha}}$.

$$\begin{aligned} \Pi_1 &= \lambda_1 \Omega_1 \\ \Pi_2 &= \lambda_2 \Omega_2 \\ \Pi_3 &= I_3 \Omega_3 + J_3(\Omega_3 + \dot{\alpha}) = \lambda_3 \Omega_3 + J_3 \dot{\alpha} \\ l_3 &= J_3(\Omega_3 + \dot{\alpha}) \end{aligned} \tag{9}$$

Applying the Legendre transformation directly to equations (8) yields the following set of Euler equations

$$\begin{aligned} \dot{\Pi}_1 &= \left(\frac{1}{I_3} - \frac{1}{\lambda_2}\right)\Pi_2 \Pi_3 - \frac{l_3 \Pi_2}{I_3} \\ \dot{\Pi}_2 &= \left(\frac{1}{\lambda_1} - \frac{1}{I_3}\right)\Pi_1 \Pi_3 + \frac{l_3 \Pi_1}{I_3} \\ \dot{\Pi}_3 &= \left(\frac{1}{\lambda_2} - \frac{1}{\lambda_1}\right)\Pi_1 \Pi_2 \end{aligned} \tag{10}$$

$$\dot{l}_3 = u \tag{11}$$

The equivalence of equations (8) and equations (10) is proved in [7].

It is interesting to note that equations (10) can also be computed using the relationship

$$\dot{\boldsymbol{\Pi}} = \boldsymbol{\Pi} \times \boldsymbol{\Omega} \tag{12}$$

which suggests that spatial momentum $\pi = \mathbf{R}\boldsymbol{\Pi}$ is conserved because

$$\dot{\pi} = \dot{\mathbf{R}}\boldsymbol{\Pi} + \mathbf{R}\dot{\boldsymbol{\Pi}} = \mathbf{R}(\boldsymbol{\Omega} \times \boldsymbol{\Pi} + \boldsymbol{\Pi} \times \boldsymbol{\Omega}) = 0 \tag{13}$$

This relationship cannot however be derived from the rigid body Lie-Poisson bracket, (described in section 4), and the kinetic energy, (or Hamiltonian $H(\boldsymbol{\Pi})$), that is computed by directly applying the Legendre transformation.

4 Stabilization about Intermediate Axis

For ease of system analysis one wants to chose the control law such that the system is conservative in sense and that the momentum spheres $\|\Pi\|^2$ are constant. In this particular case setting $\dot{l}_3 = u = k\dot{\Pi}_3$; which implies that $l_3 = k\Pi_3 + c$ where c is some constant; makes $\frac{d}{dt}\|\Pi\|^2 = 0$. Without loss of generality one can let $c = 0$ so that the closed loop equations (10) become

$$\dot{\Pi}_1 = \left(\frac{1-k}{I_3} - \frac{1}{\lambda_2}\right)\Pi_2\Pi_3$$

$$\dot{\Pi}_2 = \left(\frac{1}{\lambda_1} - \frac{1-k}{I_3}\right)\Pi_1\Pi_3 \qquad (14)$$

$$\dot{\Pi}_3 = \left(\frac{1}{\lambda_2} - \frac{1}{\lambda_1}\right)\Pi_1\Pi_2$$

$$(15)$$

The rigid body Lie-Poisson bracket is given in [6] as

$$\{F, G\} = -\mathbf{\Pi} \cdot (\nabla F \times \nabla G) \qquad (16)$$

Using this bracket and the closed loop equations (14) one can define a Hamiltonian $H(\mathbf{\Pi})$ using relationship from [6], such that the system is Hamiltonian in the Lie-Poisson structure of the reduced space $so(3)^* \simeq \mathbb{R}^3$. Explicitly the Hamiltonian must satisfy;

$$\dot{F} = \{F, H\}$$

$$\frac{d}{dt}F(\mathbf{\Pi}) = \{F, H\}$$

$$\nabla F \cdot \dot{\mathbf{\Pi}} = -\mathbf{\Pi} \cdot (\nabla F \times \nabla H) \qquad (17)$$

$$= \nabla F \cdot (\mathbf{\Pi} \times \nabla H)$$

$$\Rightarrow \dot{\mathbf{\Pi}} = \mathbf{\Pi} \times \nabla H \qquad (18)$$

One such Hamiltonian function is given by

$$H(\mathbf{\Pi}) = \frac{1}{2}\left(\frac{\Pi_1^2}{\lambda_1} + \frac{\Pi_2^2}{\lambda_2} + \frac{((1-k)\Pi_3)^2}{(1-k)I_3} + \frac{c^2}{(1-k)J_3}\right) \qquad (19)$$

As previously discussed the control was selected in order to conserve the momentum spheres $\|\Pi\|^2$. Defining a function C_Φ such that

$$C_\Phi = \Phi\left(\frac{1}{2}\|\mathbf{\Pi}\|^2\right) \qquad (20)$$

$$= \Phi\left(\frac{1}{2}(\Pi_1^2 + \Pi_2^2 + \Pi_3^2)\right) \qquad (21)$$

one can use the definition of the rigid body bracket from [6], C_I (for the case where $\Phi = I$), and an arbitrary function F to show that

$$\dot{C_I} = \{C_I, F\} = -\mathbf{\Pi} \cdot (\nabla C_I \times \nabla F) = -\mathbf{\Pi} \cdot (\mathbf{\Pi} \times \nabla F) = 0 \qquad (22)$$

This can easily be generalized for other functions Φ. This shows that functions of the form C_Φ Poisson commute with every function. This type of function is called an energy Casimir and it is clearly conserved along the flow of the system.

Using the Casimir function C_Φ and the Hamiltonian function $H(\mathbf{\Pi})$ defined in equation (19), one can prove the following Theorem from [3].

Theorem 4.1 For $k > 1 - \frac{I_3}{\lambda_2}$ and $l_3 = k\Pi_3$, the system described by equations (10) can be stabilized about its intermediate axis.

Proof Following the steps of energy Casimir method described in the introduction of [6]. The function $H_{C_\Phi} = H + C_\Phi$ has a critical point at the relative equilibrium $(0, C, 0)$ of equations (10).

Step 1 The first variation of $(H + C_\Phi)$ must vanish i.e. $\delta(H + C_\Phi) = 0$. The first variation is

$$
\begin{aligned}
\delta(H + C_\Phi) &= \Pi_1 \left(\Phi'(\frac{1}{2}\|\mathbf{\Pi}\|^2) + \frac{1}{\lambda_1} \right) \delta\Pi_1 \\
&+ \Pi_2 \left(\Phi'(\frac{1}{2}\|\mathbf{\Pi}\|^2) + \frac{1}{\lambda_2} \right) \delta\Pi_2 \\
&+ \Pi_3 \left(\Phi'(\frac{1}{2}\mathbf{\Pi}^2) + \frac{(1-k)}{I_3} \right) \delta\Pi_3 \qquad (23)
\end{aligned}
$$

Setting this equal to zero yields the following three conditions;

$$
\begin{aligned}
\Phi'(\frac{1}{2}\|\mathbf{\Pi}\|^2) + \frac{1}{\lambda_1} &= 0 \\
\Phi'(\frac{1}{2}\|\mathbf{\Pi}\|^2) + \frac{1}{\lambda_2} &= 0 \\
\Phi'(\frac{1}{2}\mathbf{\Pi}^2) + \frac{(1-k)}{I_3} &= 0 \qquad (24)
\end{aligned}
$$

Step 2 The second variation $\delta^2(H + C_\Phi)$ is

$$
\begin{aligned}
\delta^2(H + C_\Phi) &= \left(\Phi'(\frac{1}{2}\|\mathbf{\Pi}\|^2) + \frac{1}{\lambda_1} \right)(\delta\Pi_1)^2 + \\
&\quad \left(\Phi'(\frac{1}{2}\|\mathbf{\Pi}\|^2) + \frac{1}{\lambda_2} \right)(\delta\Pi_2)^2 + \\
&\quad + \left(\Phi'(\frac{1}{2}\|\mathbf{\Pi}\|^2) + \frac{(1-k)}{I_3} \right)(\delta\Pi_3)^2 \qquad (25) \\
&+ \Phi''(\frac{1}{2}\|\mathbf{\Pi}\|^2)\left(\Pi_1\delta\Pi_1 + \Pi_2\delta\Pi_2 + \Pi_3\delta\Pi_3 \right)^2
\end{aligned}
$$

6

Step 3 Definiteness Filling equation (24) into equation (25) and noting that for motion about the intermediate axis relative equilibrium of interest is $\mathbf{\Pi} = (0, C, 0)$ yields the following equation for the second variation

$$
\delta^2(H + C_\Phi) = \left(\frac{1}{\lambda_1} - \frac{1}{\lambda_2}\right)\delta\Pi_1^2 + \left(\frac{(1-k)}{I_3} - \frac{1}{\lambda_2}\right)\delta\Pi_3^2
$$
$$
+ C^2\Phi''(\frac{1}{2}\|\mathbf{\Pi}\|^2)(\delta\Pi_2)^2 \tag{26}
$$

By assumption

$$
\left(\frac{1}{\lambda_1} - \frac{1}{\lambda_2}\right) < 0
$$

since $I_1 > I_2$. Also, one can select C_Φ such that $\Phi''(\frac{1}{2}\|\mathbf{\Pi}\|^2) < 0$. Therefore for $k > 1 - \frac{I_3}{\lambda_2}$ the equation is always negative (i.e. we have sign definiteness). As such for a large enough k one can stabilize rotations about the intermediate axis.

QED

5 Simulations

In order to verify conservation of the momentum spheres $\|\Pi\|^2$ and to verify the result proved in Theorem 4.1, the system was simulated using Matlab. For the simulation the rigid carrier was described as a rectangular block with the dimensions $0.75 \times 1.0 \times 1.5$ and unity mass. The rotor was described by a cylinder a radius of 0.125, length of 0.375 and mass = 0.5. These dimensions respect the conditions $I_1 > I_2 > I_3$, $J_1 = J_2$ and $I_1 + J_1 > I_2 + J_2 > I_3 + J_3$.
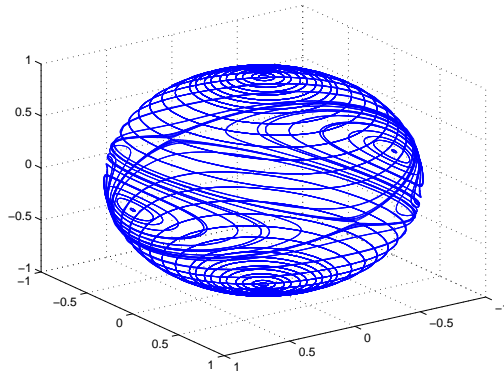

Figure 1: Stationary Rotor

Figure (1) shows the momentum sphere with $k = 0$. As expected it closely resembles the canonical picture (described in Theorem 15.9.1 of [6]), of the momentum sphere for a rigid body. As such, rotation around the (short) first and (long) third axis, the relative equilibriums $(C_1, 0, 0)$ and $(0, 0, C_3)$ is spectrally stable and rotation about the intermediate axis, the relative equilibrium $(0, C_2, 0)$ is unstable, (note C_1, C_2, C_3 are constants that define the shape of the momentum sphere). The system also respects the Hamiltonian structure in that the stable relative equilibriums are centers and the unstable relative equilibrium is a saddle, which means that there is no energy generated or lost at any point in the phase space (i.e. the volume of the phase space is conserved).
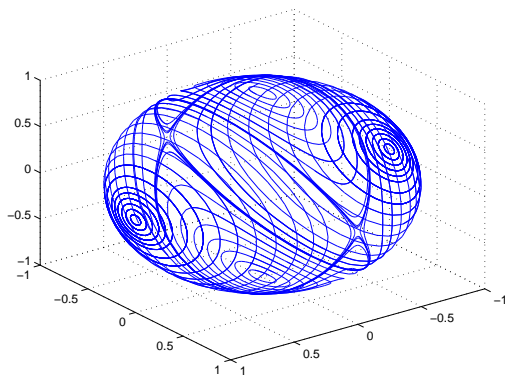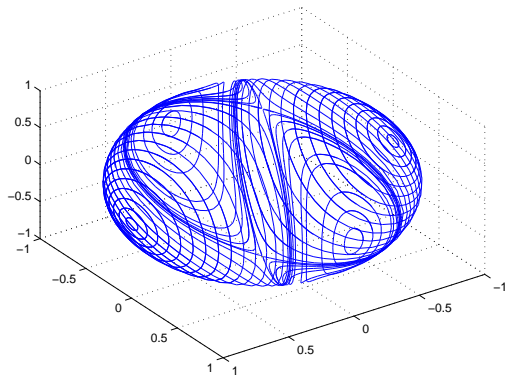

Figure 2: $\|\Pi\|_2^2$ Sphere k=0.45

Figure 3: $\|\Pi\|_2^2$ Sphere k=0.475

The critical value of $k = 1 - \frac{I_3}{\lambda_2} \simeq 0.4624$ is where the intermediate axis

stability property changes. The plots in figures (2) and (3) indicate that a bifurcation does indeed occur at this critical value of $k = 1 - \frac{I_3}{\lambda_2}$. One can see that rotation about the intermediate axis is unstable for $k = 0.45$ but for values of $k > 1 - \frac{I_3}{\lambda_2}$ as in figure (3), where $k = 0.475$, rotational stability about the intermediate axis is obtained, which verifies Theorem 4.1.

For values of $k > 1 - \frac{I_3}{\lambda_2}$, such as $k = 0.475$, the y-axis changes from the intermediate axis to the long axis and the z-axis changes from the long axis to the intermediate axis. In the resulting system the primary axis relative equilibrium $(C_1, 0, 0)$ remains an energy minimum (as described in [6]), the intermediate axis relative equilibrium $(0, C_2, 0)$ is an energy maximum and the third axis relative equilibrium $(0, 0, C_3)$ becomes a saddle.

At the critical value of k the equations of motion (eqns. 14) become degenerate as shown in equations (27).
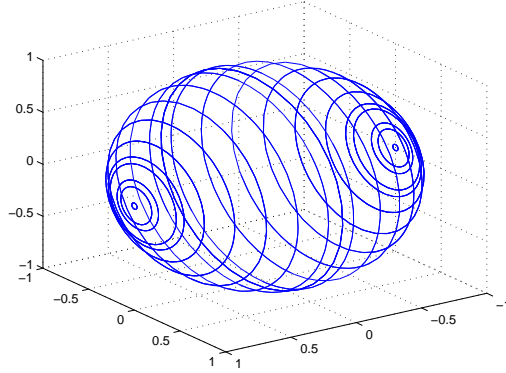

Figure 4: Critical k

$$\begin{aligned} \dot{\Pi}_1 &= 0 \\ \dot{\Pi}_2 &= \left(\frac{1}{\lambda_1} - \frac{1}{\lambda_2} \right) \Pi_1 \Pi_3 \\ \dot{\Pi}_3 &= \left(\frac{1}{\lambda_2} - \frac{1}{\lambda_1} \right) \Pi_1 \Pi_2 \end{aligned} \tag{27}$$

In these equations (27) Π_1 is clearly a constant and as such the second and third equations define the following ellipse;

$$\Pi_2^2 + \Pi_3^2 = constant. \tag{28}$$

At this point there is only one relative equilibrium $(C_1, 0, 0)$ about the x-axis. Figure (4) shows a simulation of the momentum sphere at $k = 1 - \frac{I_3}{\lambda_2}$. The simulation verifies the analysis indicating that as the equilibrium of the

9

intermediate axis transitions from being a saddle to maximum that at some critical value of k the long axis becomes the only equilibrium in the system.

It is interesting to note that there is another bifurcation that takes place around $k = 1 - \frac{I_3}{\lambda_1}$; which also indicates another degenerate point in the equations of motion; however in this case the remaining relative equilibrium is around the y-axis $(0, C_2, 0)$. Through this bifurcation the stability properties of the intermediate axis (z-axis for $k > 1 - \frac{I_3}{\lambda_2}$) and the short axis (x-axis for $k > 1 - \frac{I_3}{\lambda_1}$) are exchanged.
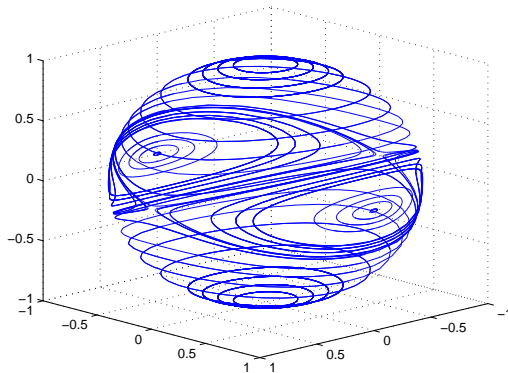

Figure 5: $\|\Pi\|_2^2$ Sphere k=1

Figure (5), which shows a simulation with $k = 1$, illustrates the resulting system. The second bifurcation results in the third axis relative equilibrium $(0, 0, C_3)$ becoming an energy minimum, the y-axis relative equilibrium $(0, C_2, 0)$ remaining an energy maximum and the x-axis relative equilibrium $(C_1, 0, 0)$ becoming a saddle. Stability of rotations about the intermediate continues for larger values up to and including $k = 100$. I did not simulate larger values of $k > 100$ for the purpose of this study. I might expect the rotations about the intermediate axis to become unstable at larger gains as the form of the control $u = k\dot{\Pi}_3$, is like a derivative action and this is known to become unstable for large gains.

6 Conclusions and Directions for Future Work

A rigid body with a rotor aligned along its third principle axis can be modeled as a Hamiltonian system. The Hamiltonian structure is derived by what is referred to in [3] as deforming the open loop equations of motion with an appropriate feedback gain and appropriate selection of the Lie-Poisson bracket. Stability of this new system can be analyzed using Energy-Momentum methods such as the Energy-Casimir method described in this report and in [6].

Simulations confirm the results obtained in [3] regarding the stabilization of rotations about the intermediate axis of a free rigid body with one rotor using a feedback system.

Also in the paper [3] the fact that the Hamiltonian structure induced by selecting the rigid body bracket to define the Lie-Poisson structure on the reduced space $so(3)^* \simeq \mathbb{R}^3$ induces a different system Lagrangian. In this new structure the new velocities for the system are $\tilde{\omega}_i = \omega_i$ for $i = 1, 2, 3$ and $\dot{\tilde{\alpha}} = \frac{\dot{\alpha}}{1-k} - \frac{k\Pi_3}{(1-k)J_3}$. This Lagrangian is quadratic in the velocities and thus defines a geodesic, study of this geodesic and the associated phase of the system would be the next step in studying the system.

Furthermore the work in this paper and specifically the derivation of the Hamiltonian for use in the energy Casimir proof of Theorem 4.1 is an example of designing a controlled Hamiltonian, this is closely related to the concept of controlled Lagrangians discussed in papers such as [5] and [4]. Another direction of future work would involve the study of these types of systems.

7   Acknowledgments

References

[1] A.M. Bloch. *Nonholonomic Mechanics and Control: Texts in Interdisciplinary Applied Mechanics, Vol. 24*. Springer-Verlag, 2nd edition, 2003.

[2] Awad El-Gohary. Optimal control of the rotational motion of a rigid body using euler parameters with the help of a rotor system. *European Journal of Mechanics and Solids*, 24:111–125, 2005.

[3] A.M. Bloch P.S Krishnaprasad J.E. Marsden and G. Sanchez De Alvarez. Stabilization of rigid body dynamics by internal and external torques. *Automatica*, 28(4):745–756, 1992.

[4] Anthony M. Bloch Naomi Ehrich Leonard Jerrold E. Marsden. Stabilization of mechanical systems using controlled lagrangians. *Proceeding Conference on Decision and Control*, 36:2356–2361, 1997.

[5] Anthony M. Bloch Naomi Ehrich Leonard Jerrold E. Marsden. Controlled lagrangians and the stabilization of mechanical systems i: The first matching theorem. *IEEE Transactions on Systems and Control*, 45:2253–2270, 2001.

[6] J.E. Marsden and T.S. Ratiu. *Introduction to Mechanics and Symmetry: Texts in Applied Mathematics, Vol. 17*. Springer-Verlag, 1994.

[7] Jerrold E. Marsden and Jurgen Scheurle. The reduced euler lagrange equations. *Fields Institute Communications*, I:139–164, 1993.